3DGEm: geological mapping for 3D geothermal exploration

Emmanuel Ramos[1], Rodney Merrill[2], Mark Linus Ramos[1], Gangerico Ramos[2]

[1]3D EDGE Corp., 309 Pacific Century Tower, Quezon Ave., Quezon City, Philippines

[2]3DGE Intl. LLC, 415 Placerville Dr., Placerville, CA, USA

[1]EmmanuelRamos@3dge.earth

ABSTRACT

3DGEm is presented as a unique and innovative tool for creating high-resolution 3D geological maps that can benefit geothermal exploration. Faint natural electromagnetic waves ae converted into two data modes: Mode A that shows EM inductance index to represent geological materials, and Mode B that displays anisotropic EM impedance coefficients whose progressive increase with depth is perturbed by faults, geological boundaries, and perhaps even temperature and permeability variations. While 3DGEm involves geophysical instruments and procedures, its two data modes portray qualitative and empirical representations of subsurface geology. The interplay between materials—mapped in Mode A, and structures—revealed in Mode B, graphically illustrates the dynamics of geothermal systems. Faults, alteration zones, perhaps even permeability and elevated temperatures, are implied by the textures and structures displayed by the impedance coefficient, whereas zones of EM inductance indices chart subsurface physicochemical features. The proxy geophysical attributes shown in 3DGEm charts reflect the geological environment to depths of a few kilometers.

Introduced in November 2024, the 3DGEm technology is currently multi-nation patent-pending. Although some permutations of its multi-sensor attributes are still to be unraveled, the simple unsupervised plots of 3DGEm data, by themselves, can already provide intuitive and highly-detailed geological models. When coupled with other field data, geothermal exploration can therefore immediately benefit from 3DGEm's high-resolution 3D geological images, without resorting to artificial intelligence, hypothetical modelling or a stretch of the imagination.

Keywords: 3D geology, electromagnetics, geothermal exploration, 3DGEm

1. INTRODUCTION

Geophysical exploration has always aimed at detection and mapping of deviations. The discovery of the Moho came from recognizing the early arrival of waves that defied the space-time pattern. Thereafter, deviations in time arrival, waveform character or space distribution of earthquake waves led to more detailed and progressively-improving image of Earth's internal structure. Electromagnetics (EM) and potential fields similarly evolved; instruments and methods improved, all honed towards detecting the smallest deviations in patterns contained by the data.

Due to its strong and detectable signals, EM energy had early analytical beginnings. Maxwell's *A Dynamical Theory of the Electromagnetic Field* (1865) describes electricity, magnetism, and light as travelling waves—launching the classical theory of electromagnetic radiation. Differential equations for electromagnetics (EM) he formulated remains uncontested, reduced to four partial differential equations by Heaviside in 1893. Faraday's lines of force explained how electric and magnetic waves are strongly coupled, and his induction theory led to creation of electric motors and generators, and prompted geophysicists to create instruments that the measured electric and magnetic parameters to estimate features and form of underlying geologic materials.

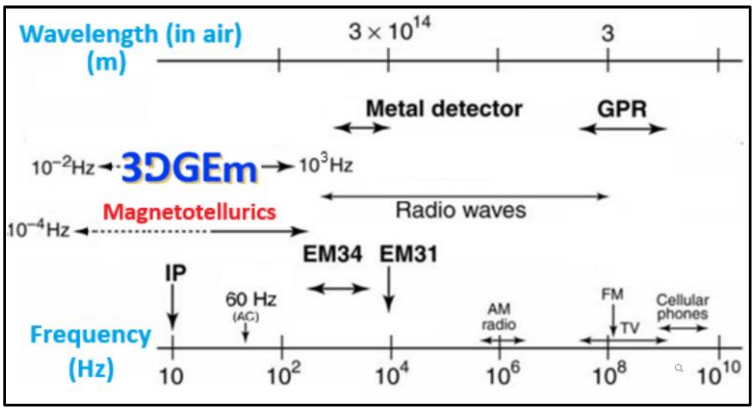

Figure 1: The spectral range of 3DGEm, extending from 0.01 Hz to 1kHz, covers a few orders of magnitude shorter than traditional magnetotellurics system.

Geophysical electromagnetics involves an amusingly large variety of instrumentation, spanning a broad range of EM frequencies (Roy, 2020). A common objective of EM instruments is to differentiate attributes of local geology from the large ambient EM signals. Polar magnetism and fierce solar storms overwhelm signals coming from underground materials. Many EM methods resorted to injected energy whose returning ground response reveal subsurface targets. Passive EM instruments, confronted by the weak geological signals, delve on improving sensor sensitivity, in minimizing noise, and in sophistication of data processing. Of late, artificial intelligence is used to create striking 3D images of the underground geology, but these flourish on dearth rather than surfeit of actual subsurface data.

In EM surveys, penetration depth is partly a function of wavelength or frequency; e.g., high frequencies used by metal detectors and GPR target the shallow sections while lower frequency systems like MT can target greater crustal depths. The 3DGEm system operates below 1 kHz,

in the lower sections of the EM spectrum (**Figure 1**) where audiometric MT operates. Conventional MT uses intricate matrix inversion algorithms to derive rock conductivity and permittivity, following Cagniard's formulation of the Maxwell's and Faraday's theories (Roy, 2020). 3DGEm skirts this indirect route, opting for correlation schemes that, although more intuitive, results in detailed and qualitative site definition, but with loss in quantitative parameters. Due to pending patent applications in several countries, certain aspects of 3DGEm's non-conventional proprietary techniques cannot yet be presented nor published.

In brief, 3DGEm embodies a system for collection, processing and visualization of data from its orthogonal electric and magnetic sensors, creating 3D outline maps of the subsurface geology. The hardware is compact and very portable; multiple units are deployed as flexible grid over the target area. Time series soundings capture ambient EM information that, when processed, reach a few kilometers below the instrument network. Straightforward data plots employ only nearest-neighbor interpolation to create coherent and geologically-rational 3D maps. This approach is similar to how seismic reflection profiles use intricate waveforms to reveal beddings, faults, contacts and other discontinuities. While sacrificing accurate measure of resistivity or magnetic strength, 3DGEm has focused on the detection of minute deviations—in both space and EM data domains—to achieve high-resolution mapping of subsurface anisotropy and heterogeneity. This article illustrates 3DGEm's charts under various geological conditions, including features that pertain to geothermal exploration.

2. METHODOLOGY/APPROACH

The frequency range of 3DGEm is shorter than MT, limiting its imaging depth to only a few kilometers. Miniature electromagnetic data recorders (**Figure 2**) use triaxial magnetometers and two horizontal electric dipoles in orthogonal geometry. Some tests used vertically-oriented electric component Ez in floating or sub-aerial platforms.



Figure 2: An array of 3DGEm instruments record the natural magnetic and electric signals for a few hours over the exploration target.

One of 3DGEm's innovation is the use of a high number of instruments in surveys. More than 20 units are commonly deployed **as** an array covering a few kilometers across, resulting in a dense 3D distribution of EM data (**Figure 3**). Noise cancellation and S/N enhancement

procedures are implemented at various stages, from field array design, style of data collection, and particularly in data processing.

3DGEm has been deployed in several surveys that covers a range of geological conditions. Deployments were in arrays that used from 10 to 25 instruments, covering areas from a few hectares to a few square kilometers in size. The system uses signal stacking. Shallow targets can take about 4 hours of recording simultaneously for all instruments, while targets of 5 kilometers depth need data that extend to 24 hours. An area of 2km by 2km can be covered by 25 instruments in a single episode while larger areas are coved by overlapping surveys. Denser instrument distribution results in finer spatial resolution.

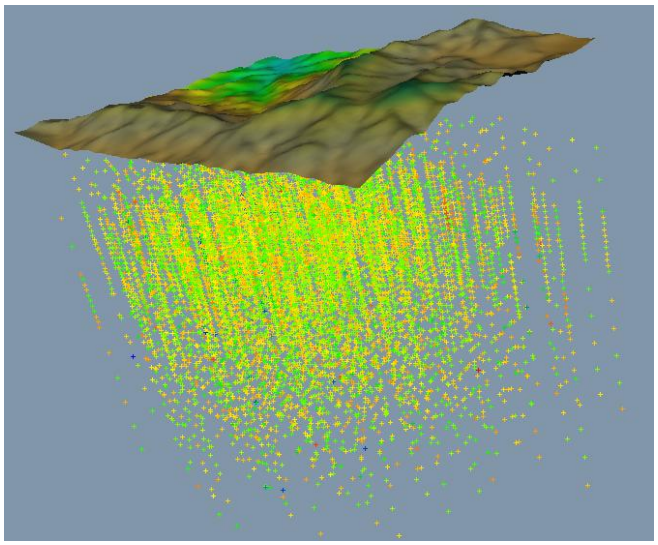

Figure 3: The multitude of 3DGEm instruments deployed in a survey creates a dense cloud of EM data from which high-resolution 3D maps are produced.

The 3DGEm data shown here were collected and processed blindly, without using *a-priori* information about the ground. In these examples, only after the initial 3D maps have been produced were the various types of external geological information called in to further evaluate or understand the site. Geological observations were made during 3DGEm surveys, as well as simultaneous collection of 2D resistivity profiles within the survey areas. Secondary data, when available, were used to correlate with the resulting charts, and to guide further data visualization and determine if such geological conditions are observed in the acquired data set. As qualitative test, 3DGEm charts were compared to the site's terrain and other surface conditions, and correlated with various forms of external data, listed in Table 1.

To remain objective, 3DGEm data are straightforward plots, and devoid of influence from artificial intelligence or numerical modelling. 3DGEm charts can only rely on its own EM data patterns in the creation of its 3D geological charts.

Table 1: External data used to validate 3DGEm.

- Outcrops
- Geological maps
- Drilling data
- Geological Models
- Google Earth data (landform)
- Topography/Geomorphology
- 3rd party Geophysical data (MT)
- Structural maps
- Tunnel observations
- Vertical ~60m deep shafts
- Cultural features of the land
- Field geologic mapping
- Geothermal models
- Cabled & VLF 2D resistivity profiles

3. RESULTS AND DISCUSSIONS

EM data is handled by 3DGEm with two separate aspects of wave propagation in mind:

A. Consistency of the EM wave properties, and
B. Disruptions caused by discontinuities

In Mode A, wave attributes (amplitude, phase, polarity, frequency, etc.) are maintained relatively consistent along a geological unit or petrofacie, allowing the medium to behave like a wave guide, and effectively mapping material heterogeneity. In Mode B, disruptions and minute deviations of the EM wave paths, caused by interfaces or property discontinuities, allows structures and anisotropy to become recognizable. Mapping wave features in Mode A reveals formation petrofacie, i.e., the subsurface material constituents, while a plot of the interfaces or discontinuities in Mode B highlights structural elements. Jointly, Modes A and B synthesizes into a composite 3D view of the overall geological setting using indexes and coefficients as proxies to EM conductivity and inductance.

3.1. Mode A: Mapping subsurface heterogeneities with inductance index

In creating Mode A charts, 3DGEm detects variations using two perpendicular magnetic and electric sensors similar to how MT charts resistivity. In contrast, however, 3DGEm focuses on finding the minute differences in measurements made between two sites, thereby mapping the inductance coefficient of the intervening region. Therefore, when the 3DGEm system maps the EM values in space, it is mapping the electrical and magnetic heterogeneity or "anomalies" in these intervening regions. This provides 3DGEM with two valuable innovations: (a) the ability to show inhomogeneities or "anomalies" as dense data cloud thereby creating high spatial resolution, and (b) the capacity to detect even the smallest of data deviations making the system sensitive to small deviations in the geological condition.

Mode A charts therefore display variations in amplitude, polarity, or phase of the EM components without regard to any theoretical derivation of a physical unit. These are therefore appreciated based on their context (e.g., **Fig. 4**). Despite Mode A charts indicating high and low values, these values are relative and unitless, and cannot be directly associated with specific geophysical unit such as conductivity or resistivity. Although tracing how 3DGEm calculates may lead to the mathematics to convert data into the familiar geophysical units, these quantifications remain peripheral to the objective of creating 3D high-resolution maps of geological significance.

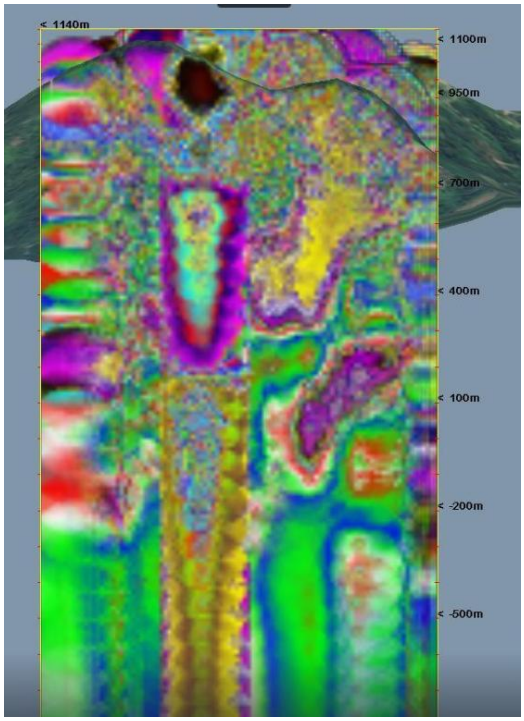

Figure 4: Mode A chart of a diatreme (center) discovered in a mineral exploration area. With Google Earth terrain on the top, the imbricated thrust faults create shallow irregular layering. Stacked colors imply vertical ore zoning as the hydrothermal fluid variably reacted with the different levels of thrusted sheets.

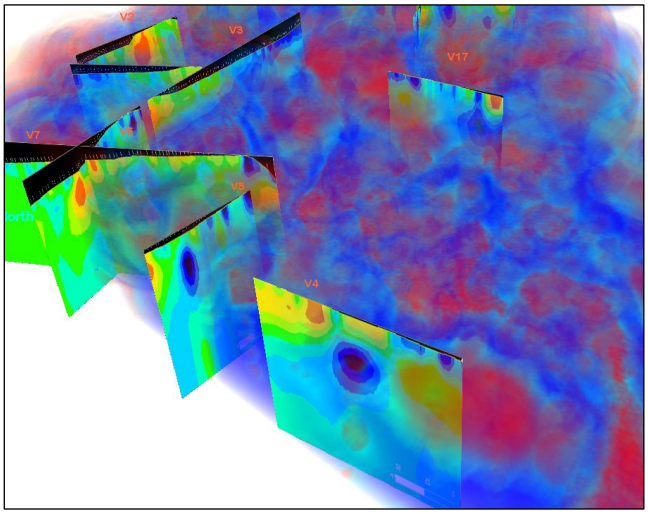

Figure 5. Perspective view from the NW of 100m thick slab of 3DGEm Mode A, as pseudo-resistivity to match the 110m-high 2D resistivity panels. (red=high, blue=low). Both 2D and 3D images show layering, erosional textures, and almost similar resistivity anomalies in this Tertiary reefal limestone area. The S end of this slab is shown in the next figure.

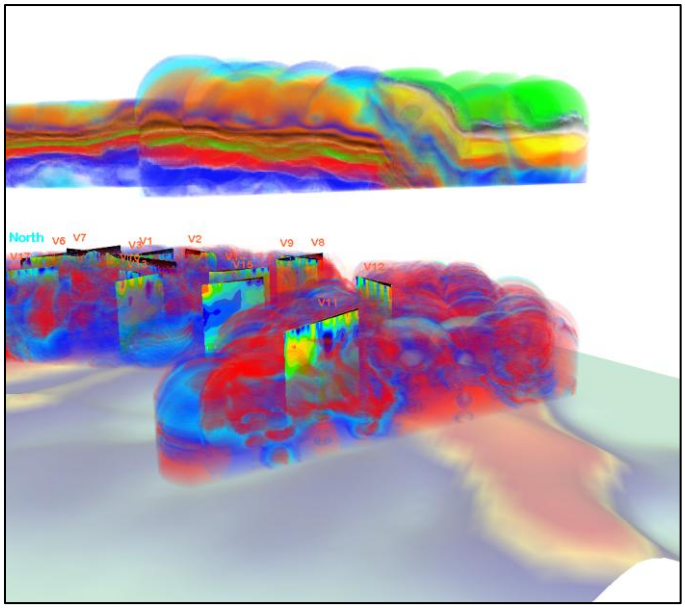

Figure 6. Simple plots of Mode A (middle) and Mode B (top) reveal ultramafic rocks (green) thrusted over the limestone beds (see **Fig. 5**). 2D resistivity panels used for data validation are visible. Terrain (bottom) shows the up-thrusted terrain. Spherical form are artifacts of interpolation at data edges.

The form of 3DGEm's Mode A maps of inductance indices may resemble typical geophysical anomaly maps, with extreme values that can be highlighted as anomalies (**Fig. 5**). However, when compared to traditional geophysical anomaly maps, the high spatial detail and fine data resolution of Mode A occur over shorter distances. For example, alteration zones create both high and low inductance index values shown as tightly-packed mixture of colorful, and pixelated zone, making such clayey horizons distinct. Some Mode A charts may also portray traditional features of a resistivity map; large homogenous zones may represent massive rock units (**Fig. 6**).

One distinct feature of 3DGEms charts, illustrated in **Figure 6**, is the intuitive nature of the images. A simple plot of Mode B data suggests the presence of a thrust fault with the hanging wall of different lithology. Later discussion with a geologist who walked the site (R. Quebral, pers. Comm 2025) validated the thrust fault and mentioned the presence of ultramafic rocks on the hill shown in the terrain.

3.2. Mode B: Using anisotropic impedance coefficients to map structures

The creation of Mode B charts follows a different concept. The natural anisotropy of inductance is shown as an index value which progressively decreases with depth. In essence, Mode B charts create a ruled, colored canvas upon which geological structures are drawn. Fault are shown to displace this color bands like how faults cut across sedimentary beds. Clastic units appear to coax the inductance index values to trace the sedimentary bedding layers. Mode B therefore effectively maps folds and dips of strata, while in non-clastic situations, the anisotropy charts show displacements and deformation caused by geological structures.

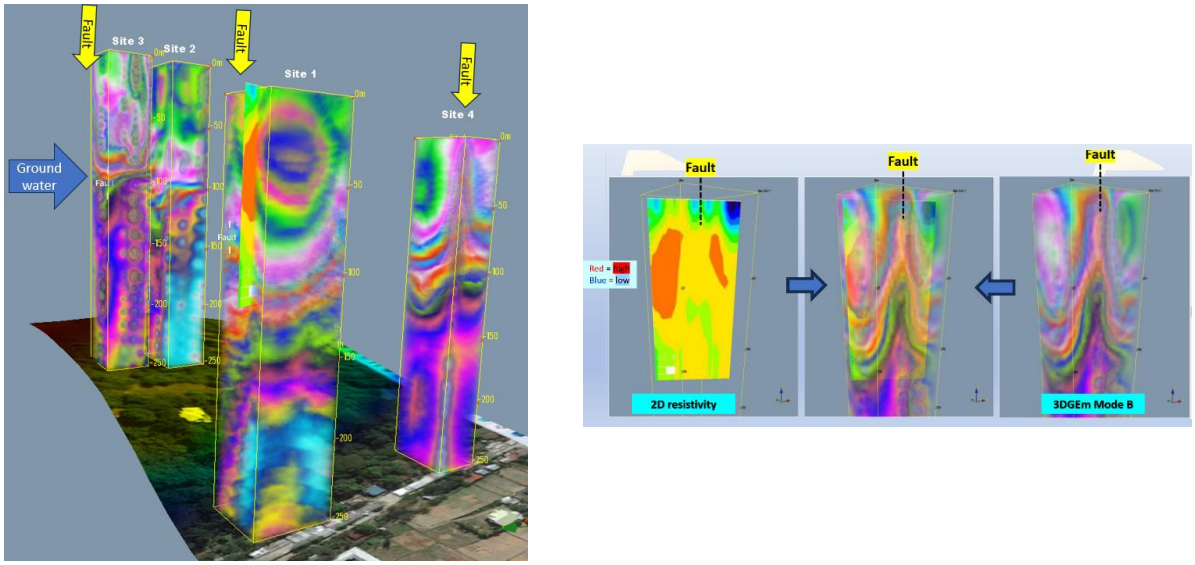

Figure 7: Four sites were surveyed to test time and space consistency of 3DGEm data. The Mode B columns show the near-horizontal conglomerate beds in all the four sites, while faults cause the vertical stretching of the signals. Groundwater level is visible, while the 50m tectonic uplift is preserved in the similarity of columns. The 2D resistivity section and its corresponding Mode B image exhibit the geometry of the vertical fault.

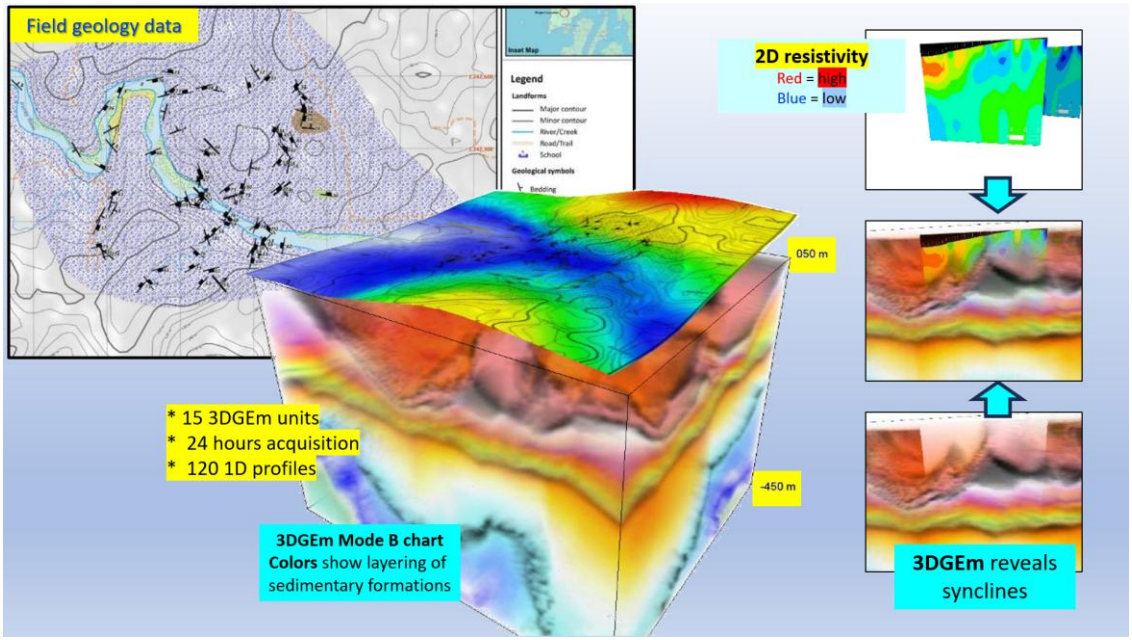

Figure 8: Sedimentary formations show irregular and shallow dip patterns (upper left) but imaged to have synclines by Mode B charts. The curved resistivity anomalies (upper right) are geometrically cradled by the folds mapped by 3DGEm (lower right).

3DGEm's geophysical information are time and space consistent over a limited district or time. **Figure 7**, for example, shows surveys conducted in four adjacent sites, the surveys separated in time by a few days, and the sites separated in horizontal and vertical space by tens of meters. The consistent result suggests that the mapped sedimentary layers can be traced from one place to another, and that even the vertical tectonic displacement of around 50m can be

tracked. The faults that crossed three of the four sites are also properly imaged, including the listric bend at depth while the groundwater level around 100m for each site is also evident. 2D resistivity profiles collected in all four sites validate the form of the EM data, while three ~60m deep vertical shafts were used to confirm the rocks, faults and groundwater level. Meanwhile, the synclines that influence the rocks and the outline of resistivity anomalies are easily mapped by Mode B charts (**Figure 8**) but missed during the detailed field mapping due to the shallow uncoordinated dips, thick soil and vegetation.

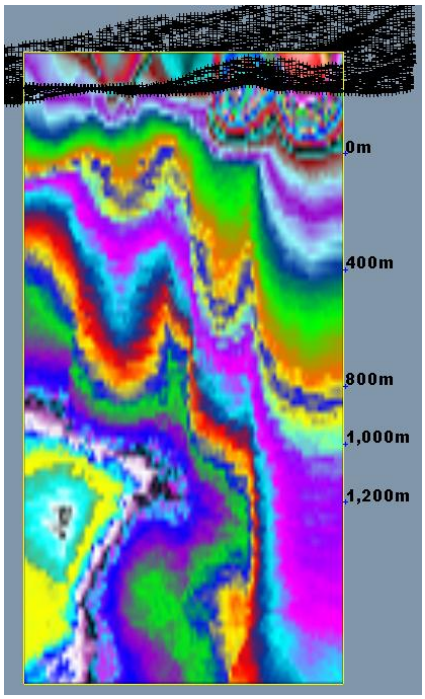

Figure 9: At least four vertical faults vividly displace Mode B bands. These structures coincide with traces of mapped faults in geological maps. The altered ground's mottled texture is also observable at the top.

Electromagnetic impedance represents the rate of flow of EM waves as a function of both resistance (opposition to flow) and reactance (opposition to change in rate of flow). In geophysics, impedance is dependent on ground conductivity and frequency. In a homogenous Earth where conductivity is constant, impedance simply becomes frequency dependent, therefore, a function of depth. 3DGEm presents a function of EM impedance using an index value that progressively decreases with depth. Mode B data therefore shows as near-horizontal color "bands" whose vertical anisotropy is perturbed by geologic structures. For instance, Mode B's impedance index bands follow sedimentary layering, capturing the dips of beds, and the folds and irregularities in geological layers (**Figure 8**). Likewise, faults and other abrupt geological discontinuities show as structural disruption in the Mode B bands. The charts of impedance index therefore appear like sedimentary layers that vividly display the geological structure, be it bedding or faults.

Mode B value bands seem to also respond to water table, permeability, fluid activity, and apparently, temperature. Compared to Mode A whose mapped form are context dependent, Mode B data's graphical image of structures renders the colored bands of Mode B values to act like ruled paper upon which the geologic structures are drawn (**Figs. 8** and **9**).

3.3. 3DGEm charts in a geothermal area

It is observable that 3DGEm's charts are context-driven, and their significance can take various forms. This is like geophysical anomaly maps that lack a legend. 3DGEm charts are therefore analyzed based on the survey site and objectives. In **Figures 5** and **6**, Mode A charted electrical a proxy of resistivity, while in **Figure 7** it shows the position of the water table. In a different context, various grades of ore may be imaged (**Fig. 4**). This context-driven analysis applies well in geothermal exploration where the complex geological environment is deciphered piecemeal through a collection of 3DGEm images may have varied meanings. The vertical and inclined faults shown in **Figure 10** can be interpreted to contain geothermal fluids and not ore only because these are related to a geothermal reservoir.

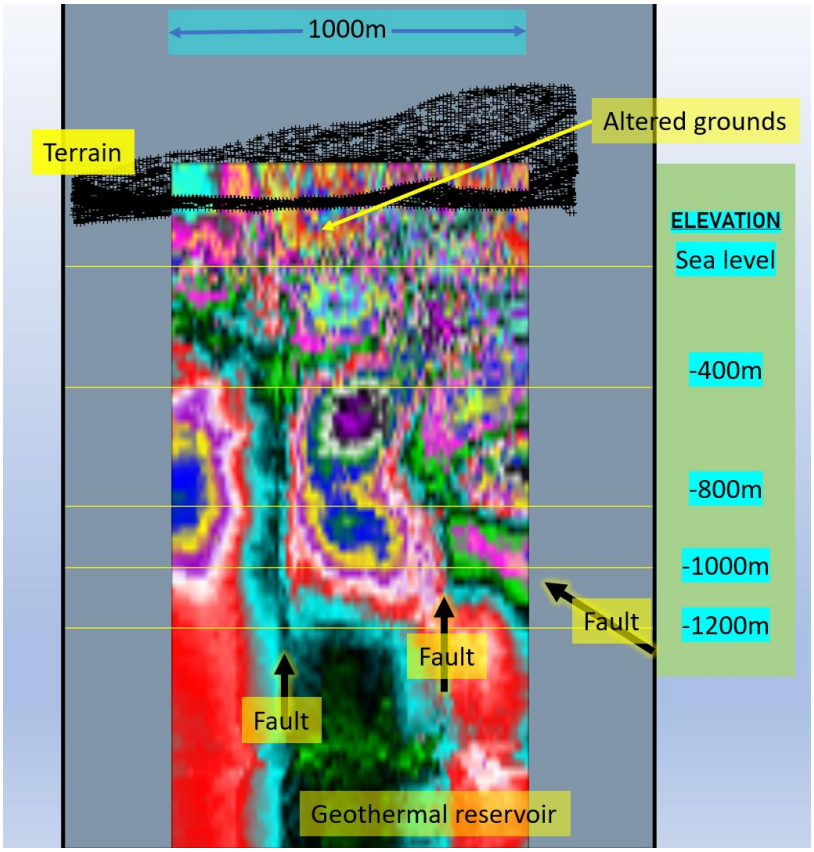

Figure 10: Faults shown in Mode A are interpreted to contain geothermal fluids, and may be recharge structures if linked to a surface drainage, or a channel for hot brine if connected to the heat source. By association, the altered ground on top is easily associated with the distinct mottled texture.

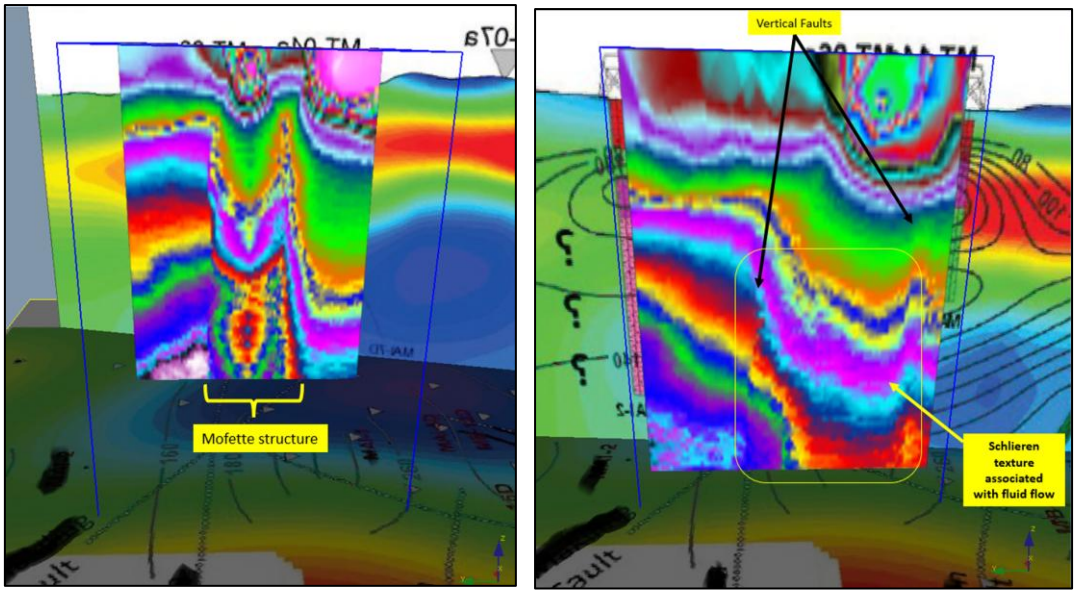

Figure 11: Structures that may be peculiar to geothermal areas include mofette structures (left) and Schlieren texture (center) that suggest diatreme and fluid activity, respectively. Mode B bands are also observed to sag around the geothermal reservoir.

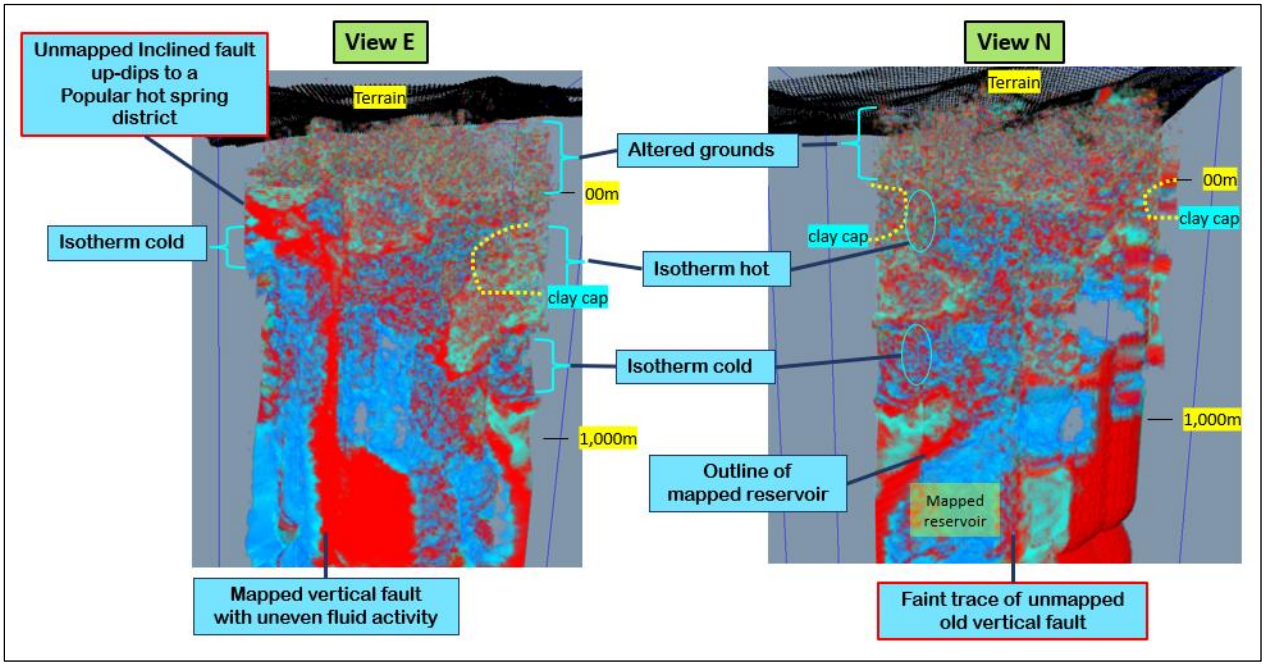

Figure 12: Hydrothermal fluids as inferred from Mode A data, viewed looking E and N. Sketched in for correlation are geothermal features earlier defined from MT surveys, geological mapping, and well drilling. Vertical faults coincide with those in geologic maps, while two unmapped, possibly older faults (red-borders), are suggested by Mode A data. Interpolation artifacts show as spherical edges at the lower right.

Certain features seen in 3DGEm charts can be exclusively associated with geothermal activity. The presence of mofette structures (**Figure 11**), being suggestive of recent fumarolic activity, were found in the vicinity of the geothermal reservoir that we have mapped. These structures are not only occurring as single structures, but may be multiples

or nested. Interestingly, these diatremes usually display with depressed centers, highlighting the crater form of the structure.

It can also be observed from **Figures 9** and **11** that the downward sag of Mode B impedance index bands is not confined within the narrow margins of the fumaroles, but may extend over an area that seems to follow the outline of the geothermal reservoir. This sagging of the Mode B bands can therefore be inferred to arise from the lower electrical impedance and magnetic strength at these heated zones.

Another interesting phenomenon seen in both the Modes A and B images is the presence of Schlieren texture around the area of the reservoir (**Figs. 9** & **11**). Visually seen as vertical smearing of the colored patches or bands, the Schlieren texture tend to smudge the item boundaries and visually suggests that thermal activity or migrating fluids may be involved. This can then be interpreted to have permeability implications, if supported by evidence from other data.

The 3DGEm images provide visual links between structures and the identified geothermal reservoir show, therefore allowing the implied thermal fluids to be digitally isolated from the other elements as shown in **Figure 12**. This chart then suggests a 3D model of the of the geothermal fluid circulation. The role of the vertical fault in channeling heated waters into the surface is evident, even as this may also interact with shallower features and lead to the altered grounds on the surface. Also, the presence of an inclined SE-dipping fault is revealed, and seem to act as a major influence in the plumbing of geothermal fluids. Interestingly, the activity along both the previously-mapped vertical fault and the newly-discovered inclined fault seems discontinuous; only selected portions of these faults seem to contain fluids and thus their traces are not continuous.

The vertical distribution of the red-colored texture in **Figure 12** also reveals a possible zonation in the bulk hydrogeology, where more dense but smaller fluid features are on the top, a less dense feature follows at mid depth, and a sparse zone of fluid features are seen at the reservoir level. The geothermal features observed from MT and drillholes are also sketched into the **Figure 12** charts, and their position seem to be related to different textural zones. Interestingly, aside from the noticeable vertical zone of textures, the light blue color, leading up from the mapped reservoir, suggest a roughly-helical feature that contrasts with the greenish-blue zones. Whether this relates to any observable geothermal feature is yet to be proven.

4. SUMMARY AND CONCLUSIONS

Geothermal sites are a complex mixture of rocks and fluids traversed by faults and volcanogenic structures, and further complicated by ongoing chemical and thermal activity. In this environment, a rational approach for greenfield exploration is first to visualize the structures that may influence hydrothermal activity, then trace if geologic materials can be linked to these structures to support a conceptual model. This approach allows the structures to frame the logic on why geologic materials are in certain locations. Faults (seen in Mode B) can be probed if these contain fluids (seen in Mode A) and be connected to streams on the surface thus suggesting recharge, or to hotsprings thus suggesting upflow. This interplay

between the Mode B structures and the Mode A materials can be used suggest a rational geologic model that explains the geothermal field. Furthermore, certain structural features seem unique to geothermal systems and guide the search for the heat source. In all these stages, the critical use of corroborating geological and geophysical data is imperative.

3DGEm is primarily an enhanced terrestrial visualization system for geothermal and mineral exploration. Its capabilities for high-resolution characterization of structural elements and petrofacies offer the following benefits and advantages:

- Passive, nodal, portable, stand-alone instrumentation
- Flexible duration of field measurements, a few hours to few days
- Efficient and fast data reduction schemes (proprietary)
- High resolution 3D visualizations
- Cost-competitive integrated service, from field to graphical realizations

The above-described field cases demonstrate the versatility of the 3DGEm system to elucidate subsurface geological morphologies. It provides spatially-detailed composite 3D visualizations at resolutions surpassing other surface-based geophysical techniques. Viewing Modes A and B reveal the intricate details in the architecture, structural elements, and geological units; which are then easily correlated with other client in-house interpretations (such as seismic sections, MT surveys, borehole logs, analogues, etc). Integrating 3DGEm visuals with others leads to an improved understanding and appreciation of dynamic interactions between hydrothermal fluids and host formations, thereby guiding informed resource management decision-making processes.

With its broadening applications and user base, coupled with emerging device miniaturization and data-manipulation technologies, 3DGEm is poised for further refinements in geothermal tomography.

ACKNOWLEDGEMENTS

Surveys using 3DGEm were generously allowed by a number of anonymous entities. We deeply thank them for the privilege of using their sites to probe how 3DGEm can image the subsurface.

REFERENCES

Heaviside, Oliver (1893). Electromagnetic Theory. Vol. 1. The Electrician Printing and Publishing Co, London. ISBN 978-0-8284-0235-4

Maxwell, James Clerk (1861). "On physical lines of force". Philosophical Magazine.

Maxwell, James Clerk (1865). "A dynamical theory of the electromagnetic field". Philosophical Transactions of the Royal Society of London. 155: 459–512.

Roy, Kalyan. (2020). Natural Electromagnetic Fields in Pure and Applied Geophysics. 10.1007/978-3-030-38097-7.